5 PBPK modelling for pharmacokinetic simulation and pharmacodynamic evaluation of the RLZ ASD

5.1 Background of the study

RLZ is a neuroprotective, anti-excitatory agent which is the only approved drug by US FDA for ALS for oral drug delivery [231]. The human dose of this drug is 100 mg/day (50 mg twice a day), which attenuates the disease progression including a favorable risk to benefit ratio [158,232,233]. Clinical trials (approx. 18 months) have shown that RLZ can extend survival time of 2-3 months with a 43% reduction in death rate. But the major challenge for RLZ is drug-induced liver injury (DILI), associated with increased alanine aminotransferase (ALT) and aspartate aminotransferase (AST) levels and low bioavailability leading to reduced on-site efficacy. Neutropenia is another condition for which healthcare providers must be vigilant [234]. The mean absolute oral bioavailability for RLZ is reported to be approximately 60%. A solubility as low as 0.3 mg/ml at neutral pH makes its oral bioavailability dissolution rate limited [235].

To overcome the issue of hepatic toxicity, a better understanding of PK is required which can be done by utilizing a physiologically based pharmacokinetic (PBPK) model. PBPK are mathematical models which incorporate physiological and biochemical parameters to predict concentration-time profiles in different organs. PBPK models give an edge in estimating the pharmacokinetic (PK) profile of a substance based on its preclinical ADME data and estimating the exposure in a target organ following drug administration by taking into account the rate of absorption and disposition in that organ as well as metabolism within that organ, if applicable [236].

5.1.1 Plan of work

The objective of this work was to i) develop an amorphous solid dispersion of RLZ for

enhanced solubility and bioavailability, ii) conduct animal experiments for generating PK profile for RLZ ASD and marketed formulation iii) develop a PBPK model for rat and human to evaluate on-site efficacy and off-site toxicity, and iv) evaluate the RLZ ASD for its effect on cognitive functions against the marketed tablet Rilutor™ (Sun Pharma Industries Ltd. Batch No. JMC0745A) and RLZ API in male wistar rats. The model validation was done by extracting the clinical data on humans from published literature.

5.2 Experimental section

5.2.1 Preparation of amorphous solid dispersion of RLZ

ASD was prepared employing rapid solvent evaporation technique in a rotary evaporator (IKA RV 10 auto pro V). 1:1 ratio of methanol and dichloromethane were taken for dissolving RLZ and PAA in different weight ratios (30:70, 20:80 and 10:90) under constant stirring. The prepared solution was then evaporated under vacuum at a bath temperature of 55 ^{o}C and a vacuum gradient of 500 mBar to 2 mBar was gradually applied. The ASDs were dried in a vacuum oven for 24 hours at 25 ^{o}C in order to eliminate any remaining solvent. The samples were passed through ASTM #100 and stored at 4 ^{o}C.

5.2.2 Solid-state Characterization

5.2.2.1 Powder X-Ray Diffraction Study

PXRD study of different ratio of RLZ:PAA ASD was evaluated under Rigaku Miniflex 600 X-ray diffractometer at ambient temperature. Monochromatic Cu K radiation at 100 mA and 40 kV in the vicinity of 5°-50° scanned at 5^{o}/min with an angular increase of 0.02°/s were used for the study.

5.2.2.2 Differential Scanning Calorimetry Study

To examine the thermal behavior of the prepared ASD, the samples were analyzed under DSC. Sample weighing approximately 3-5 mg was taken in crimped aluminium pans and heated under DSC from –40 ºC-140 ºC at a scan rate of 20 ºC/min. Nitrogen purge at a rate of 50ml/min was maintained throughout the DSC runs.

5.2.2.3 Transmission Electron Microscopy

For TEM studies, homogenous solutions of different ratio of drug and polymer in the 1:1 DCM: methanol mixture were prepared, and spin coated on 200 mesh carbon coated copper grid. Bright field images and selected area electron diffraction (SAED) pattern were captured on TecnaiG2T20 TEM operating at 200 kV for analyzing the samples.

5.2.3 High Performance Liquid Chromatography Method Development and Validation

For quantitative analysis of drug in various studies a HPLC system (Waters Milliford, USA) connected to a Photodiode Array (PDA) detector (model 2998, Waters, USA) ,a LCsystem consisting of a binary pump (model 1525; Waters, USA), a manual injector valve with20 µL loop, and C18 column (150 mm*4 mm; 5 um) was utilized. The injection volume of 20 µL was taken and sample detection was done at a wavelength of 264 nm. The mobile phase constituted acetonitrile: water in a ratio of 65:35 and 1 ml/min flow rate. The analysis run time was 10 min. The Breeze program was utilized to carry out the data acquisition.

5.2.4 Biopharmaceutical Performance Evaluation

5.2.4.1 Saturation solubility study

The solubility of RLZ in different media was evaluated using the shake flask method. Media with different pH (1.2, and 6.8) and biorelevant media *viz.* fasted simulated gastric fluid (FaSSGF) and fasted simulated intestinal fluid (FaSSIF) were used for the study. The solubility study was done using shake flask method for 72 hours at 37±0.5 ^{o}C. In a 100 ml volumetric flask, 50 mL of the media and about 100 mg of RLZ were added. After 24, 48, and 72 hours, samples were taken out, filtered through 0.2 um filters, diluted appropriately, and then subjected to an HPLC analysis. The study was done in triplicate and mean values are reported.

5.2.4.2 In vitro dissolution testing

The dissolution of RLZ from ASD versus Rilutor™ was evaluated employing USP type-II apparatus (Electrolab India Pvt Ltd.). 900 mL of 0.1 N HCl (pH 1.2) and FaSSGF were used for the dissolution experiments, which were carried out at 37.0± 0.5 °C with a paddle rotating at a speed of 50 rpm. Rilutor™ tablets and RLZ ASDs equivalent to 50 mg RLZ were filled inside hard gelatin capsules and added to each vessel. 5 mL samples were taken at set intervals (5, 15, 30, 45, 60, 90, and 120 min). The volume was kept constant by adding fresh media in an equal amount. HPLC method as described above was used for the RLZ concentration determination. The study was done in triplicate and mean values are reported.

5.2.4.3 Plasma and brain pharmacokinetics in male rats

All the experiments were conducted in accordance with the approved study protocol (IIT(BHU)/IAEC/2022/010). Adult male Wistar rats were kept in standard laboratory conditions and were provided with a standard pellet meal and water. The rats were

randomly divided into two groups, each consisting of four animals. The first group received RLZ-PAA ASD, while the second group received crushed Rilutor™ of RLZ at a dose equivalent to 10 mg/kg, administered orally via oral gavage. Before administration, each formulation was prepared by suspending it in a 0.5% w/w solution of carboxymethyl cellulose. Blood samples were collected from the retro-orbital route at specific time intervals: 0, 0.25, 0.5, 1, 2, 3, 6, and 12 hours, in heparinized micro-centrifuge tubes. Immediately after blood collection, plasma was separated by centrifugation at 7000 rpm for 5 minutes at 4°C. The supernatant plasma was separated using a micropipette and stored at -20^{o} C until further processing.

To study the brain kinetics thirty rats were divided into two groups. Each rat received oral doseequivalent to 10 mg/Kg RLZ-PAA ASD and crushed Rilutor™ of RLZ. Three animals each at 0.5, 1, 2, 6 and 12 hours were killed for brain extraction. For brain homogenate preparation, the brain was weighed accurately and homogenized with 1:5 w/v of 50% v/v aqueous acetonitrile.The brain tissue sample was then centrifuged at 10000 rpm for 10 min and the supernatant was collected. Samples of brain homogenate samples were stored at –80 ^{o}C until further analysis. The control blank plasma and brain was drawn from rats before dosing, processed and stored until analysis.

For the preparation of the calibration curve 90 µl of a biological sample (plasma or brain homogenate) was spiked with 10 µl of working solutions ultimately producing a drug concentration ranging from 20-2000 ng/ml. 100 µl of the biological sample was taken and 100 µl of ACN to facilitate protein precipitation. The mixture was vortexed for 1 min and then centrifuged at 10000 rpm for 10 mins. 100 µl of supernatant was collected and subjected to heating at 80 ^{o}C under constant nitrogen purge. The residue was then reconstituted with 100 µl solution of 5- methoxypsoralen in a concentration of 20 µg/ml and vortexed further for 5 min. The resultant solution was then injected into HPLC for

drug quantification set at the parameter described above.

5.2.5 Literature Data Extraction for PBPK modeling

5.2.5.1 Rat Literature Experimental Data

Data were extracted from a study by Ravi *et al*. where an oral dose of 10 mg/Kg BW was administered to male Wistar rats weighing 180-220 gm [237]. Plasma samples were analyzed at 0.25, 0.5, 1, 2, 3, 4, 6, 8, 12, and 16 h post dose and analysed using HPLC method. Webplotdigitizer was used for extracting the data for all literature studies [238].

5.2.5.2 Human Literature Experimental Data

To check PBPK model predictions, the clinical data done on humans were extracted from different literature. There were three independent studies in the literature where RLZ tablet formulation was administered to the human population and plasma samples were quantified. The first study was from Liboux *et al*.where an oral dose of 100 mg was given and plasma samples were quantified at different timepoints [239]. Another study was from Chandu *et al.* where one 50 mg tablet was given to 54 healthy volunteers with 240 ml of drinking water. Blood samples were collected, and plasma was analyzed by LC-ESI-MS/MS [240]. The third study was taken from Longo *et al*. where 50 mg RLZ tablet during phase I study were administered and plasma concentration for 24 hours were quantified [241].

5.2.5.3 Development and optimization of the PBPK model

Perfusion-limited PBPK model with 9 compartments *viz*., stomach, gut, liver, brain, kidney, lungs, fat, heart, rest body and plasma were developed considering Rilutor™ and ASD formulation (Figure 5.1). The exchange of drug between blood and tissue in each organ is governed by blood flow also called as perfusion limited or flow limited

model. The model was developed in rats due to availability of literature and in-house data and later extrapolated to humans which can be helpful in guiding clinical studies. Oral dosing was considered through gut using first order rate constant. The unbound or free fraction (fu) was considered available for distribution, metabolism and excretion from the body.

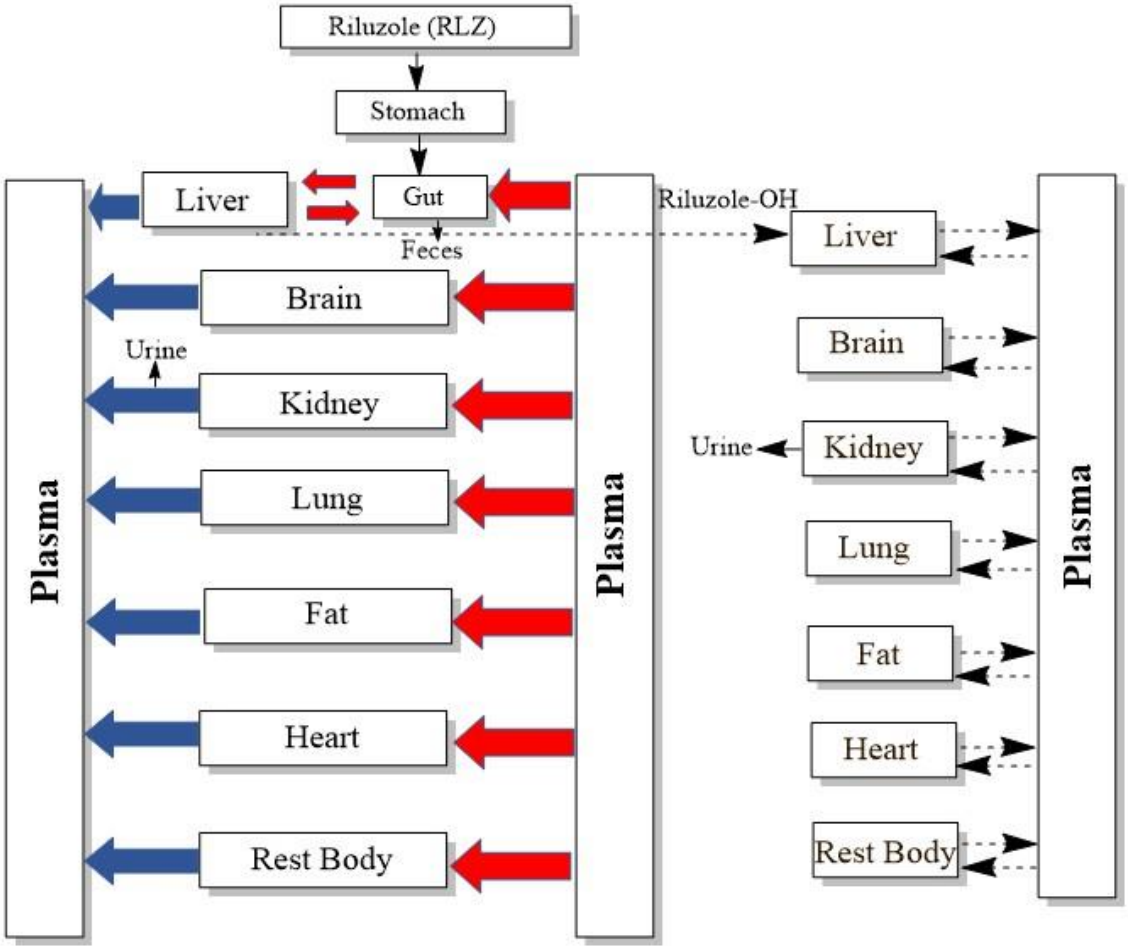

Figure 5.1. Nine compartment PBPK Model with excretion from urine and feces. The model was used to predict concentration-time profile in different compartments. RLZ-OH is being represented by dotted lines

Distribution of drug from one compartment to another was controlled by partition coefficient along with blood flow. The partition coefficient of RLZ was taken from literature (wherever data available) for specific organs and for remaining organs with no data availability, QSAR (Quantitative structure activity relationship) model was used.

Partition coefficient was calculated using Rodger and Rowland approach for perfusion-limited model [242].The R script for Rodger and Rowland approach has been provided on GITHUB for users and also can be referred through the published literature [243]. The elimination of the drug was through metabolism in liver and excretion using urine and feces from the kidney and gut respectively. There are six major and multiple minor metabolites of RLZ which are mostly metabolized in liver by hydroxylation and glucuronidation catalyzed by cytochrome P450 enzyme [244]. Among all metabolizing enzymes, CYP1A2 is majorly involved in RLZ clearance followed by UGT1A1. The major metabolite, N-hydroxy RLZ (RLZ-OH) generated with CYP1A2 enzyme was considered for this study. RLZ metabolism was described through Michaelis-Menten kinetics with parameters like V_{max} and k_m using equation 5.1.

$$V_{met} = \frac{V_{max} * C_{liver} * f_u}{K_m + C_{liver} * f_u} \qquad \text{Equation 5.1}$$

The absorption parameters like gastric emptying, absorption rate constant, and bile rate constant were optimized based on experimental data. Fraction unbound (fu) was extracted from literature [244]. Renal clearance was taken from Longo *et al*. 2020 [241] where it was calculated by data extracted from Liboux *et al*. 1997 [239]. Fecal elimination was optimized considering 90% absorption in human [241]. The *in vivo data* by Ravi *et al.* 2012 was used for optimization of the parameters for the tablet formulation. In case of ASD, only three parameters which mainly reflect the biopharmaceutical component were changed (i.e., gut absorption rate constant, undissolved drug in feces, and bile rate constant). The detailed equation for PBPK has been provided in the next section.

The model developed for rats of Rilutor™ and ASD was extrapolated to humans without any variation in the model structure. The rat physiological parameters were replaced

with human-specific parameters. For the biochemical parameters, the highly accepted allometric scaling based on body weight was used (provided in equation 5.2) [245]. In equation 5.2, param refers to biochemical parameters which were scaled, and AE to allometric exponential value. Finally, a PBPK model for human was developed by adjusting the gastric emptying rate (GE) and keeping rest parameters similar. Different dosing scenarios at 50 and 100 mg were used for checking the prediction of the model with the observed data. The input parameters i.e., physiological and biochemical are mentioned in Table 5.1.

$$Param = Param * (\frac{BW\_human}{BW\_rat})^{AE}$$ Equation 5.2

Table 5.1. Physiological and biochemical parameters used for rat and human PBPK Model

Parameters	Value in Rat for Rilutor™, ASD	Reference
Blood flow to Organ (Fraction of cardiac output)		
Liver	0.174	[246]
Lung	0.021	[247]
Kidney	0.141	[248]
Heart	0.051	[245]
Brain	0.02	[245]
Fat	0.07	[249]
Volume of Organ (Fraction of BW)		
Liver	0.036	[248,249]
Lung	0.006	[248]
Kidney	0.0073	[249,250]
Heart	0.004	[250]
Brain	0.006	[248,249]
Fat	0.07	[249]
Plasma	0.074	[249]
Biochemical Parameters		
Liver:Plasma	2.2	Taken from literature[a]
Brain:Plasma	2.44	Experimental[b]

Parameters	Value in Rat for Rilutor™, ASD	Reference
Kidney:Plasma	4.622509	Calculated using R&R[e]
Lung:Plasma	5.958539	Calculated using R&R[e]
Fat:Plasma	14.12276	Calculated using R&R[e]
Heart:Plasma	4.251126	Calculated using R&R[e]
GE ($1/hr/kg^{0.25}$)	2.61	Optimized*
Kabs ($1/hr/kg^{0.25}$)	0.69, 2.19	Optimized*
Fu (unitless)	0.04	Experimental[c]
FuM1 (unitless)	0.04	Considered similar as parent compound.
V_{max} ($nmol/h/kg^{0.75}$)	250000	Optimized*
K_m (µmol/l)	140	Optimized*
Cl_{urine} ($µl/hr/kg^{0.25}$)	0.3771	Taken from Literature[d]
$ClM1_{urine}$ ($µl/hr/kg^{0.25}$)	0.3771	Considered similar as parent compound.
K_{feces} ($1/hr/kg^{0.25}$)	0.013, 0.011	Optimized*
Blood flow to Organ (Fraction)		
Liver	0.257	[251]
Lung	0.034	[250]
Kidney	0.177	[251]
Heart	0.09	[252]
Brain	0.117	[247]
Fat	0.052	[251]
Volume of Organ (Fraction)		
Liver	0.026	[248,251]
Lung	0.014	[248,253]
Kidney	0.004	[248]
Heart	0.012	[252]
Brain	0.021	[248,250]
Fat	0.187	[248]
Plasma	0.03976	[247]
Biochemical Parameters		
Liver:Plasma	2.2	Similar to Rat
Brain:Plasma	2.44	Similar to Rat
Kidney:Plasma	4.622509	Similar to Rat
Lung:Plasma	5.958539	Similar to Rat
Fat:Plasma	14.12276	Similar to Rat

Parameters	Value in Rat for Rilutor™, ASD	Reference
Heart:Plasma	4.251126	Similar to Rat
GE ($1/hr/kg^{0.25}$)	2.61	Optimized*
Kabs ($1/hr/kg^{0.25}$)	0.69, 2.19	Similar to Rat
Fu (unitless)	0.04	Similar to Rat
FuM1 (unitless)	0.04	Considered similar as parent compound.
V_{max} ($nmol/h/kg^{0.75}$)	250000	Similar to Rat
K_m (µmol/l)	140	Similar to Rat
Cl_{urine} ($µl/hr/kg^{0.25}$)	0.3771	Similar to Rat
$ClM1_{urine}$ ($µl/hr/kg^{0.25}$)	0.3771	Considered similar as parent compound.
Kfeces ($1/hr/kg^{0.25}$)	0.013, 0.011	Similar to Rat

[a]Longo *et al.* reported liver:blood partition coefficient of 2.0, with RLZ blood to plasma ratio of 1.1. Hence liver:plasma partition was considered 2.2 [241].
[b]Calculated using AUC_{brain} from mice study at 10 mg/kg [254].
[c] [244]
[d] [241]. Calculated renal clearance using data from Liboux *et al.*
[e] [242]
*Optimized based on experimental data from Ravi *et al.* [237] in Rilutor™ and for ASD using our in- house data for rat. For human, data from Liboux *et al*. [239] was used to optimize gastric emptying.

5.2.5.4 Model Optimization

Prior distribution was provided for specific biochemical parameters based on the Longo *et al*. [241]. Optimization for tablet PBPK model was done by data from Ravi *et al*. and for ASD by our in-house data. In case of human PBPK, only one parameter was optimized based on data from Liboux *et al*. Markov Chain Monte Carlo (MCMC) simulation was performed to optimize the parameters. MCMC simulation helped in narrowing the range of the optimized parameters. Later some of the parameters were also fitted visually to get good prediction and improve goodness-of-fit [255].

Table 5.2. Prior distribution of biochemical parameters for MCMC. Prior distribution was set based on literature knowledge about RLZ

Parameter	Prior Distribution
Gastric Emptying	0.7-4
Kabs	0.5-10
Vmax	0.1e+2 - 0.1e+8
Km	0.1e+1 - 0.1e+8
kfeces	0.001-0.9
Krestbody : plasma	0.01-10
Bile rate constant	1-50

5.2.5.5 Model evaluation and Local Sensitivity Analysis

To validate the accuracy of our model predictions, a calibrated rat model using both in house *in vivo* data and rat data obtained from Ravi *et al*. 2012 [237] was employed. By comparing the plasma and brain concentration-time profiles generated by our model with the observed data, the model's predictive capabilities were accessed. The calibrated rat model was used to check the model prediction using in house *in vivo* data and therat data from Ravi *et al*. The plasma and brain concentration-time profile were checked and compared with observed data. PBPK model in human was evaluated with data from multiple case studies [239,240,256]. The PK parameters C_{max}, T_{max}, $AUC_{0\text{-}t}$, were calculated and compared for both simulated and observed data.

A normalized local sensitivity analysis was performed to examine the influence of biochemicalmodel parameter on the model output (equation 5.3) [245]. In eq.3, NSC stands for normalized sensitivity coefficient, inc refers to increase in AUC or parameter value and ori refers to original value for the AUC or parameter. Each parameter was increased by 1% to evaluate the change in plasma AUC.

$$NSC = \frac{(AUC_{inc} - AUC_{ori})/AUC_{ori}}{(Param_{inc} - Param_{ori})/Param_{ori}} \qquad \text{Equation 5.3}$$

The PBPK model was coded in MCSIM (Version 6.1.0) under Rstudio (Version 4.2.1).

5.2.6 Pharmacodynamic evaluation

5.2.6.1 Drugs and treatment

For the investigation of cognitive function, male Wister rats weighing 150–200 g were used. Each polyacrylic cage held six rats and was maintained at a controlled temperature of 25 ± 2 °C and humidity of 50 ± 10% with a 12-hour light/dark cycle. Prior to the experiment, the animals were allowed unlimited access to food and water and had a week to acclimatise. The behavioural testing was held an hour before the food was withheld. The Institutional Animal Ethics Committee of Banaras Hindu University, Varanasi, India, authorised the experimental protocols (IIT(BHU)/IAEC/2023/II/004).

The animals were divided into seven groups with six animals in each group. For the study these groups; I) Control group (saline) II) Scopolamine (SCO) 5mg/Kg III) SCO+ Donepezile (DNZ) 5mg/Kg IV) SCO+ RLZ ASD (5 mg/Kg) V) SCO+ RLZ ASD (10 mg/Kg) VI) SCO+ Rilutor™ (10 mg/Kg). DNZ and SCO were freshly dissolved in distilled water, and investigational compounds were suspended in 0.5% sodium carboxymethyl cellulose (SCMC) immediately before dosing. SCO was delivered via intraperitoneal injection (i.p.), while other compounds were administered orally (p.o.) using an oral gavage. The administration period spanned seven days, with SCO given solely on the seventh day to induce amnesia. Behavioral tests were conducted 30 minutes post-SCO administration [257].

5.2.6.2 Morris Water Maze Test

The Morris Water Maze (MWM) consisted of a water-filled, black, circular pool with dimensions of 120 cm in diameter and 25 cm in height. The pool was split into four sections, with a concealed platform in the middle of each target quadrant that was just below the water's surface (15 cm in diameter). During the trials, the platform's location

remained unchanged. A video camera positioned above the pool's centre tracked the animal's movements. Before the training rats were accustomed to swimming in the maze for 60 seconds without the platform.

Rats were trained to locate the hidden platform for five days in a row during the acquisition phase. Four trials were performed in each session, lasting 60 seconds each with a 15-second break in between. The rats were placed in the pool facing the wall and were allowed to search for the submerged platform for 60 seconds. After this the rats were allowed to remain on the platform for another 20 sceonds and remember the spatial cues. During each trial the animal were released in the different qudrant of the pool, but the platform remained in the same position. The escape latency (delay to identify the platform) were measured for acquisition assessment. Spatial reference memory was assessed on day six, seven and eight using the same procedure as training period [258]. All the recordings were done by a blind observer.

5.2.6.3 Biochemical parameter estimation and evaluation of hepatotoxicity

Blood samples of rats from group I, IV, V, VI and VII were collected after 24 hours of last day of dosing. Plasma was collected after centrifugation of blood at 7000 rpm for 5 mins. The level of enzyme was estimated using commercial kits following their protocol. For histopathology evaluation liver was extracted from the rats after killing them. The slides were prepared and analysed for hepatotoxicity in the liver tissue.

5.2.6.4 Statistical analysis

The results are expressed in mean with standard deviation. The data were analysed by Graph Pad Prism Software for windows (Version 5.0) using two-way ANOVA.

5.3 Results and Discussion

5.3.1 Solid-state Characterization

5.3.1.1 Powder X-Ray Diffraction Study

It is a widely used technique to determine the composition of the sample and the crystal structure. As seen in Figure 5.2a, the pure crystalline form of RLZ showed sharp and distinct peaks at 2θ values of 9.14, 13.64^{o}, 18.18^{o}, 22.74^{o}, and 25.22^{o} demonstrating the crystalline nature of RLZ. However, the ASD of RLZ prepared with all the aforementioned ratios *viz*. 10:90, 20:80 and 30:70 RLZ: PAA ASD showed a complete absence of Bragg peaks. the broad weak peaks denote the amorphous nature of the prepared ASD in all the ratios.Thus, the XRD study confirms the successful preparation of RLZ ASDs with polymer PAA.

5.3.1.2 Differential Scanning Calorimetry Study

DSC is a thermal technique that explains the physical properties of the drug molecule and the prepared formulations. In Figure 5.2b, the DSC thermogram of pure crystalline RLZ, and ASDprepared with different drug and polymer ratios *viz.* 10:90, 20:80 and 30:70 RLZ: PAA ASD are shown. The sharp endothermic peak occurring at 120 ^{o}C corresponds to the melting point of RLZ hence demonstrating the crystalline nature of RLZ [259]. The other thermograms of theprepared ASDs show the absence of sharp endothermic peaks, this is a clear indication of the amorphization of the drug. Hence, the successful preparation of the ASDs of RLZ with PAA is confirmed. No sharp endothermic peaks were observed in any of the ASD formulation confirming complete amorphization of the drug [259]. However, 10:90 RLZ:PAA ASD showed highest change in specific heat indicating more stable amorphous state

5.3.1.3 Transmission Electron Microscopy

The bright field images from multiple areas of the prepared sample were captured, as shown in Figure 5.2c.The likelihood of forming any crystalline phase is very less as the morphology of the particle dictates to be spherical in the image. The SAED pattern (Figure 5.2d) of the captured region exhibited diffused rings and complete absence of any systematic spot or array indicates the presence of an amorphous solid with complete absence of any crystalline particles. This suggests the formation of ASD with homogenous continuous phase [124] [260]

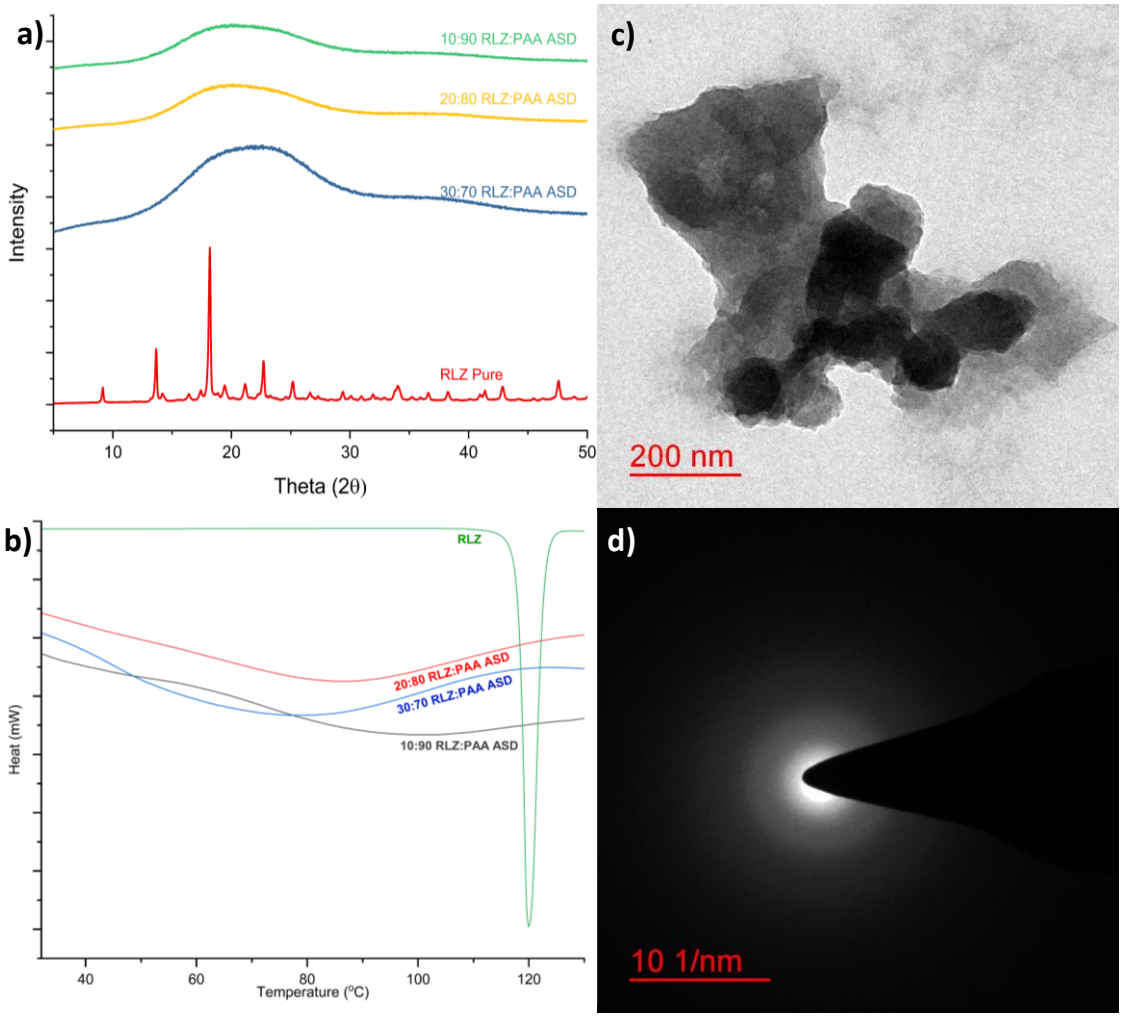

Figure 5.2 a) XRD Plot of ASD prepared with different ratio of RLZ and PAA in comparison with pure crystalline RLZ b) DSC thermogram of RLZ, and RLZ: PAA ASD prepared with different drug and polymer ratio c) TEM image of the optimized ASD formulation and d) SAED pattern of optimized ASD formulation

5.3.2 High performance Liquid Chromatography (HPLC)

The chromatograms of *in vitro* and *in vivo* analysis of RLZ are shown in figure 5.3. RLZ showed a peak at 3.9 mins in organic solvent. The details have been mentioned in table 5.2.

Table 5.3. Results of HPLC method validation for *in vitro* and *in vivo* analysis

Parameter	***In vitro***	**Plasma**	**Brain**
Retention time (min)	3.9	4.6 (RLZ) and 4.2 (5-MS)	4.6 (RLZ) and 4.2 (5-MS)
Linearity and Range		**Method validation**	
a. Calibration range		20-2000 ng/ml	
b. R^2 value	0.9996	0.9979	0.9962
c. Slope	71171±284	9801±285	8683±198
d. Intercept	-14043±46	1824±142	4912±163
Accuracy (% Recovery)	95.2-105.6%	97.3-107.9%	96.5-106.3%
Precision (% RSD)			
a. Interday	4.08%	2.46%	3.97
b. Intraday	4.39%	2.84%	6.09
LOD	1.17	0.3	0.1
LOQ	1.51	0.9	0.3

Values represented as mean on n=6±SD

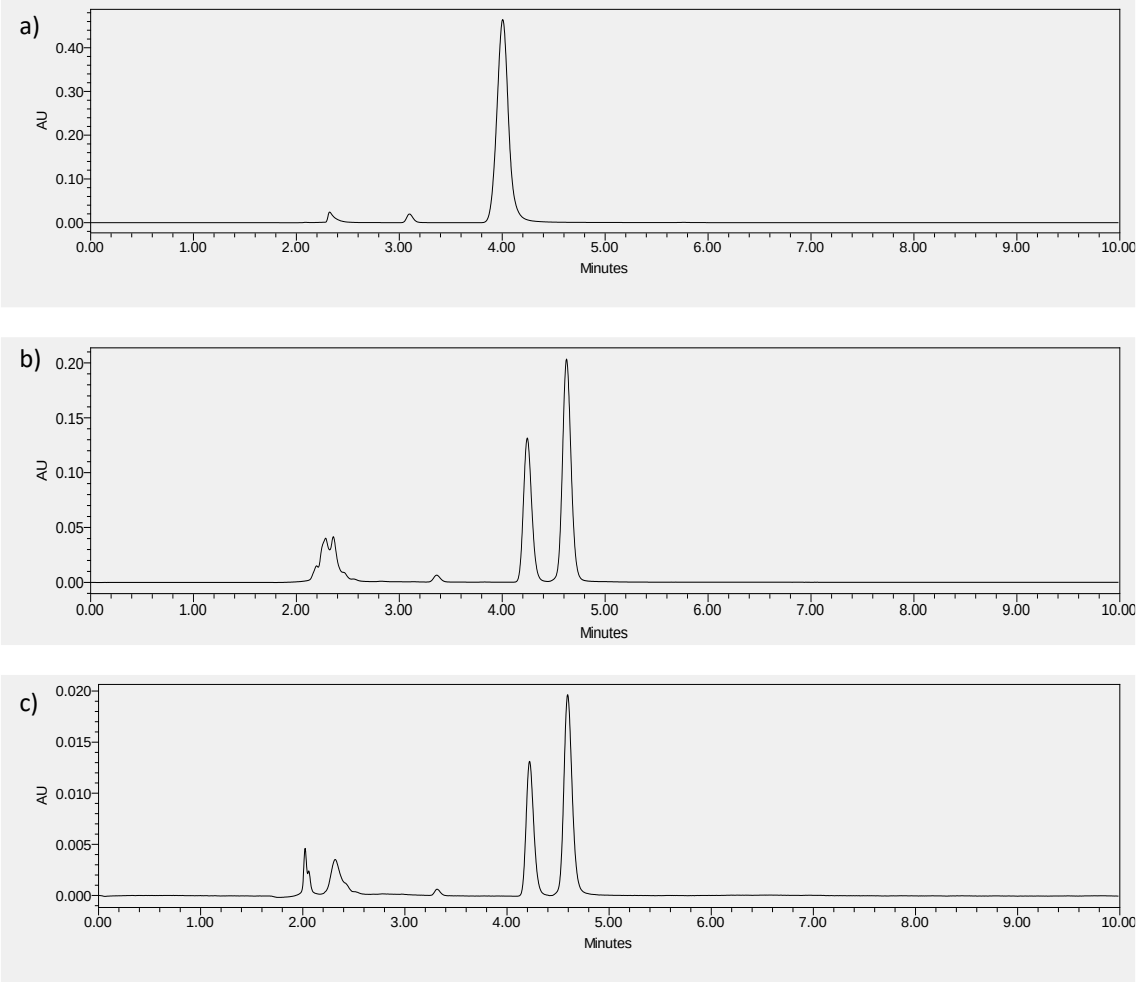

Figure 5.3. HPLC chromatogram of RLZ in a) ACN b) plasma and c) brain

5.3.3 Biopharmaceutical performance evaluation

5.3.3.1 Saturation solubility study

RLZ is a fluorine containing weakly basic compound with a dissociation constant of 3.47. The solubility was observed to be pH-dependent as it showed solubility of 12.43 mg/ml at acidic pH of 1.2 and very low solubility of 0.33 mg/ml at pH 6.8. The solubility of RLZ in FaSSGF and FaSSIF was slightly higher than pH 1.2 and pH 6.8, respectively. Hence, RLZ demonstrated higher solubility at pH 1.2 than pH 6.8. The solubility data of RLZ in different media is shown in figure 5.4a. the RLZ solubility at pH 1.2 and FaSSGF was multiple folds higher than its solubility at pH 6.8 and FaSSIF, hence the *in vitro* dissolution studies at pH 6.8 and FaSSIF was ruled out for further studies. The saturation

solubility data is also supported by Handerson-Haselbalch equation in which pH 1.2 facilitates 99.5% ionization of RLZ while pH 6.8 facilitates only 0.05% ionization [261]. Also, RLZ has an absorption site of upper gastrointestinal tract [262] hence, dissolution at pH 1.2 and FaSSGF was more relevant.

5.3.3.2 In vitro dissolution testing

Figure 5.4 b and c show the dissolution profile of the marketed tablet of RLZ i.e., Rilutor™ and ASD RLZ: PAA in different ratio 30:70, 20:80, and 10:90. As seen in the dissolution profile at pH 1.2 in the initial 30 mins all the ASD formulations showed 100% drug release while Rilutor™ showed 68% drug release. All the ASD formulations showed their maximum release of drug, and the profile became superimposable from the initial 60 mins of the dissolution except for Rilutor™. It was due to the relatively lower solubility of the crystalline RLZ present in Rilutor™. All the three ratios of RLZ ASD resulted in substantially enhanced dissolution profile, where10:90 RLZ: PAA ASD had the highest rate of drug release hence it was chosen for conducting further studies. The higher rate of drug release in FaSSGF than at pH 1.2 could be due to the surfactants present in the biorelevant media [263,264]. The enhanced dissolution profile of 10:90 RLZ:PAA ASD over the other ASDs can be explained based on the phenomena of dissolution of ASDs being polymer-controlled at lower drug loadings [265]. PAA is a water-soluble polymer, hence the higher polymer concentration leads to higher drug dissolution. Additionally, water induced amorphous-amorphous phase separation could be a reason of lower drug release with subsequent increase in the drug loading [266]**.** It is mentioned in other studies as well that PAA which is an anionic polymer shows ionic interactions with weakly basic drugs which result in a dramatic decrease in molecular mobility and hence decreased crystallization propensity of the drug [188].

Additionally, model-independent similarity factor (f_2) of 35, 29 and 23, for 30:70, 20:80 and 10:90 RLZ:PAA ASD respectively, give evidence of dissimilarity in the dissolution profile of ASD formulations with respect to Rilutor™. Dissolution profile of Rilutor™ in FaSSGF was 75% after 60 min and complete release was observed at 120 min of dissolution study. In FaSSGF RLZ:PAA 10:90 ASD showed complete release after 45 mins while RLZ:PAA 20:80 ASD and RLZ:PAA 30:70 ASD showed complete release after 60 min. Calculated f_2 value of 43, 38 and 33 for 30:70, 20:80 and 10:90 RLZ:PAA ASD respectively with respect to Rilutor™, proves the difference in their dissolution profile.

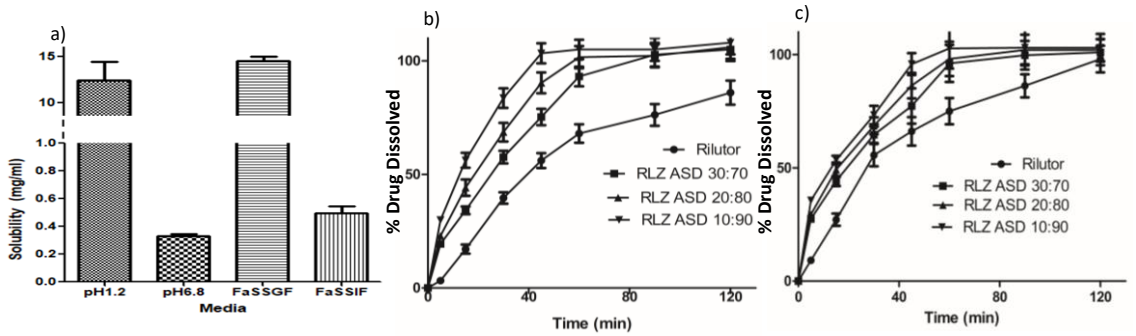

Figure 5.4. a) Saturation solubility plot of RLZ in different media, *in vitro* dissolution profile of RLZ PAA ASD in the ratio 10:90, 20:80 and 30:70 in comparison with Rilutor™ b) at pH 1.2 c) in FaSSGF. Vertical bars represents the standard deviation of mean values of n=3.

5.3.3.3 Plasma and brain pharmacokinetics in male rats

The concentration of RLZ in plasma and brain after administering single dose of 10 mg/Kg is shown in figure 5.5a and b. A substantial increase in the C_{max}, AUC and relative bioavailability (F_{rel}) was observed in case of RLZ ASD with respect to the marketed tablet formulation. The pharmacokinetic parameters of RLZ are shown in table 5.4.

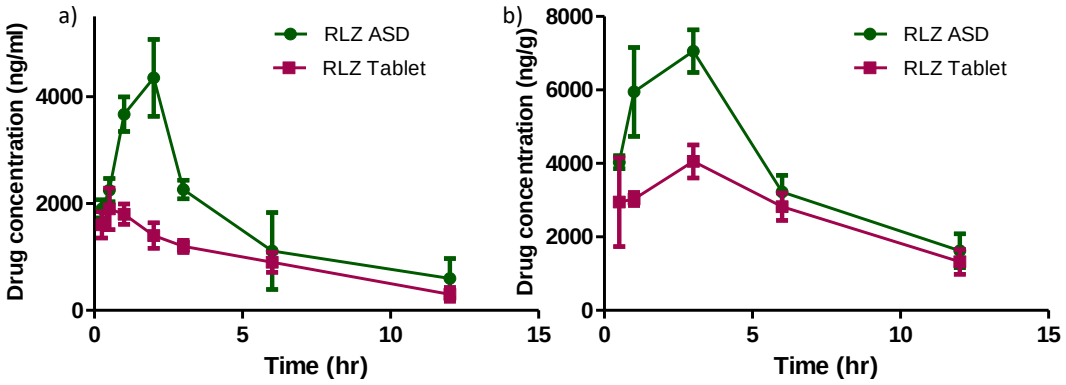

Figure 5.5. Concentration-time profile of RLZ ASD vs RLZ Tablet a) in plasma b) in brain. Vertical bars represent the standard deviation for mean value of n=4

Table 5.4. Pharmacokinetic Parameters of RLZ ASD vs Rilutor™

Tissue	Parameters	Tablet	RLZ ASD	F_{rel}
Plasma	AUC_{0-12} (ng/ml*hr)	10866.17±2432	19188.04±2854**	176%
	C_{max} (ng/ml)	1900±130	4350±243**	
	T_{max} (hr)	0.87±0.09	1.26±0.18**	
Brain	AUC_{0-12} (ng/g*hr)	31700.72±3578	55093.55±4984***	173%
	C_{max} (ng/g)	4050±196	7050±187***	
	T_{max} (hr)	1.98±0.22	2.14±0.31**	

(p<0.001), *(p<0.0001)
Data is represented in n=4±SD

5.3.4 Rat PBPK model

5.3.4.1 Plasma and brain concentrations for Rilutor™

Rat PBPK model was used for the simulation of the single dose of 10 mg/kg BW/day after oral administration. Figure 5.6a showed a simulated plasma concentration-time profile for 24 hours with blue line, black line, and red line representing percentile 2.5, median, and 97.5, respectively, along with experimental data in red circle from Ravi *et al*. 2012 [237]. It can be seen that the simulated details are quite close to the observed data at all time points. Figure 5.6b shows the plasma and brain profile at 10 mg/Kg BW/day of our in-house data. Simulated data is within the range of 1.5-2-fold of observed data points for both organs. The simulation reasonably captured the plasma and brain PK of RLZ for the available dosing scenario, however, the model needs to be further evaluated

for different dosing scenarios. To the best of our knowledge, no such study in literature was found for rats at a dose other than 10 mg/Kg for tablet. Nonetheless, the model provides a starting point for predicting the PK in different dosing scenarios.

5.3.4.2 Simulated vs observed plasma and brain concentrations

The simulated plasma and brain concentration for a single 10 mg/Kg ASD formulation of RLZ is shown in Figure 5.6c along with the observed data points from our in-house data. For optimization, only plasma concentration was used. The model was reasonably able to capture the brain PK as well.

Notably, the simulated and observed C_{max} in brain for ASD (Simulated: 5965.075, observed: 7050 ng/g) was 2-3 times higher than Rilutor™ (Simulated: 3072.61, Observed: 4050 ng/g). AUC was also higher for ASD formulation (Simulated brain: 26532.5, observed brain: 31700.72 ng/ml*hr) compared to Rilutor™ (Simulated brain: 40044.3, Observed brain: 55093.55 ng/ml*hr) in both plasma (Table 5.4) and brain pointing towards increased efficacy of the formulation.

Table 5.5. Simulated and observed AUC and C_{max} of tablet and ASD for rat in plasma and brain at 10 mg/Kg

Percentile	Simulated (Plasma)	Observed (Plasma)	Simulated (Brain)	Observed (Brain)
AUC_{0-24} Tablet (ng/ml*hr)	12221.55	10866.17	26532.5	31700.72
AUC_{0-24} ASD (ng/ml*hr)	18422.9	19188.04	40044.3	55093.55
C_{max} Tablet (ng/ml and ng/g)	1855.77	1900	3072.61	4050
C_{max} ASD (ng/ml and ng/g)	4095.5	4350	5965.075	7050

5.3.5 Human PBPK Model

5.3.5.1 Plasma and brain concentration-time curve for tablet

The simulated and observed plasma concentrations for a single 50 mg and 100 mg tablet exposure of RLZ are shown in Figure 5.7b. The simulated C_{max} and AUC were within 2.5

and 97.5 percentile of the observed data obtained from clinical trials for 50 and 100 mg from Liboux *et al.* 1997 [239] and Chandu *et al*. 2010 [240]. Increase in the plasma concentration in a dose dependent manner was observed for the Rilutor™. As the 50 mg data was not used for optimization, it was used independently for model validation. The model was also able to explain other published data from Longo *et al*. 2020 at 50 mg (Figure 5.7a).

In the ASD PBPK, concentration of RLZ in the brain for ASD is higher than the concentration in the brain for Rilutor™ (Figure 5.7c). As expected, C_{max} for ASD was about 2-2.5 times higher compared to the tablet and for the brain AUC as well, a similar trend was observed. This suggests that the overall dosing can be reduced to achieve a similar concentration in the brain as Rilutor™, hence reducing the toxicity of RLZ. This can be highly helpful for patients who suffer from RLZ adverse effects due to high-dose administration. In future, this model can be further evaluated with clinical data from ASD formulation.

5.3.6 Local sensitivity analysis for rat and humans

Figure 5.8a shows local sensitivity analysis for rat PBPK at 10 mg/Kg BW tablet. It was found that the rest body: plasma partition coefficient was highly sensitive followed by the liver: plasma partition coefficient, V_{max}, k_m, and fu. In the case of ASD, V_{max}, and k_m were highly sensitive towards AUC plasma (Figure 5.8b). This can be due to increased dissolution and absorption in ASD formulation, as a result, more drug is available in plasma and liver, so metabolic parameters became sensitive due to the limitation of CYP enzymes. This can be one of the reasons for the sensitivity of the liver: plasma partition coefficient. Fu was also sensitive, and the rest of other parameters were less than 0.5 (sensitivity coefficient). For the human, Rilutor™, and ASD PBPK model, liver: plasma

partition coefficient was highly sensitive parameter suggesting that increase in partition coefficient will decrease the plasma AUC (Figure 5.8c, 5.8d). This can be possible since more drug present in liver will lead to an increased metabolism and hence reduced AUC in plasma. Fu, V_{max} are also highly sensitive parameter. Another interesting fact is that for human Rilutor™, urinary clearance and fecal elimination were sensitive whereas they were not so sensitive parameters for ASD formulation.

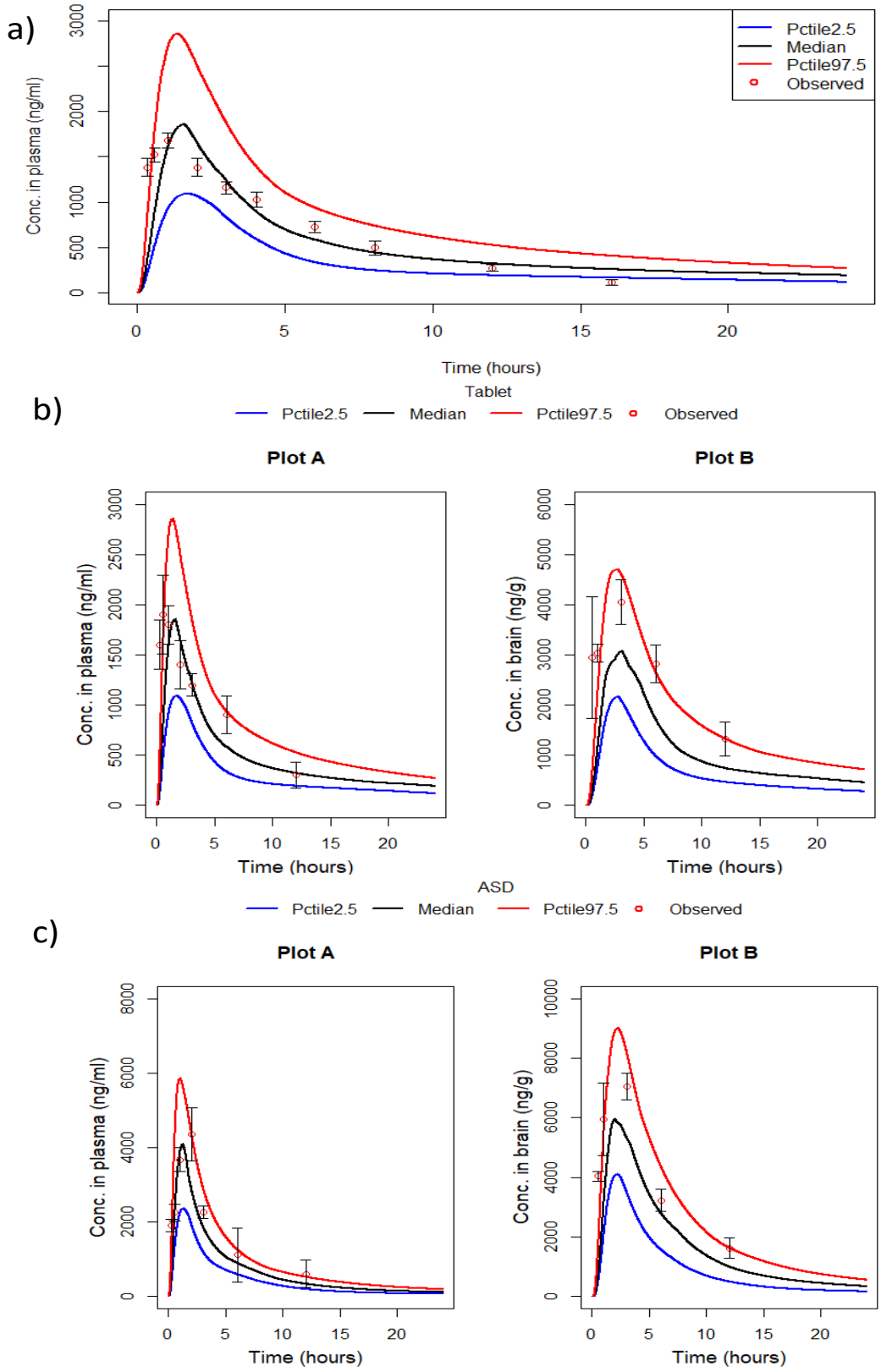

Figure 5.6. Concentration-time curve in rats a) plasma for Rilutor™ after 10 mg/Kg BW exposure b) for plasma (Plot A) and brain (Plot B) after dosing of 10 mg/Kg BW c) for plasma (Plot A) and brain (Plot B) after dosing of 10 mg/Kg BW ASD formulation; The blue line, black line and red line represents the 2.5th percentile, median, and 97.5th percentile, respectively. Red circles accompanied by bar represent the mean and SD from our in-house rat data

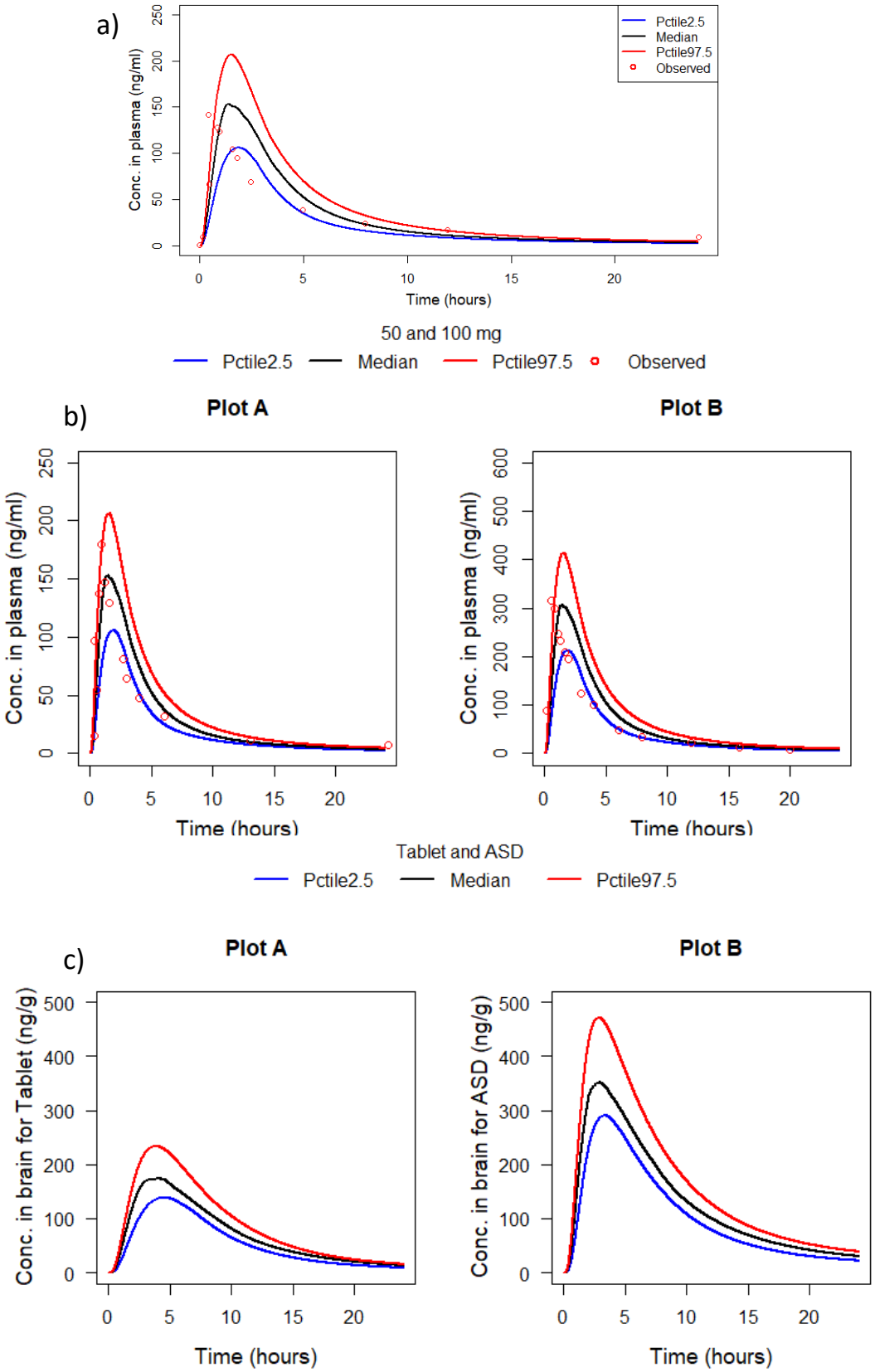

Figure 5.7. Concentration-time curve in a) plasma after dosing of 50 mg tablet per day b) plasma at the dosing of 50 mg (Plot A) and 100 mg (Plot B). Experimental data extracted data from Liboux *et al*. and Chandu *et al.* is represented by red circles c) for brain at 50 mg dosing for Rilutor™ (Plot A) and ASD (Plot B); The blue line, black line and red line represents the 2.5th percentile, median and 97.5th percentile, respectively

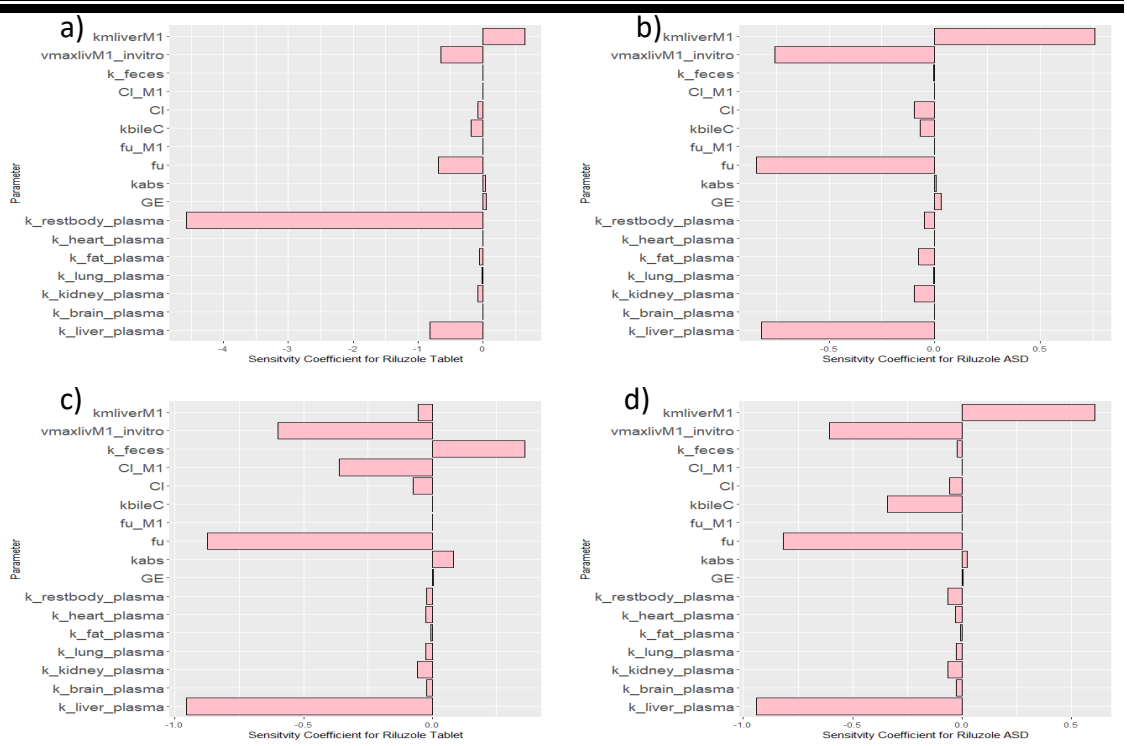

Figure 5.8. Local sensitivity analysis of a) Rilutor™ b) Riluzole ASD using rat PBPK at 10 mg/Kg BW/day dose c) Rilutor™ d) Riluzole ASD using human PBPK at 50 mg/day dose

5.3.7 Pharmacodynamic evaluation

5.3.7.1 Morris water maze test

The learning and memory tests were conducted using the Morris water maze test. Throughout the training sessions of five days, the average time rats taken for rats to escape reduced steadily. However, group II (which served as the negative control) took longer to locate the platform (as shown in Figure 5.9). After the training session of five days, the escape latency was measure for each rat in each group on day 6, 7, and 8. In figure 5.8 it can be seen that the escape latency time for group IV was less than the group III and V. It can be simply explained on the basis of enhanced relative bioavailability of RLZ ASD at the same dose with respect to Rilutor™. Group III with RLZ ASD at 5mg/kg is also performing better, this can be used as a indication for dose reduction in future treatment which will exert the same therapeutic effect but show little side effect.

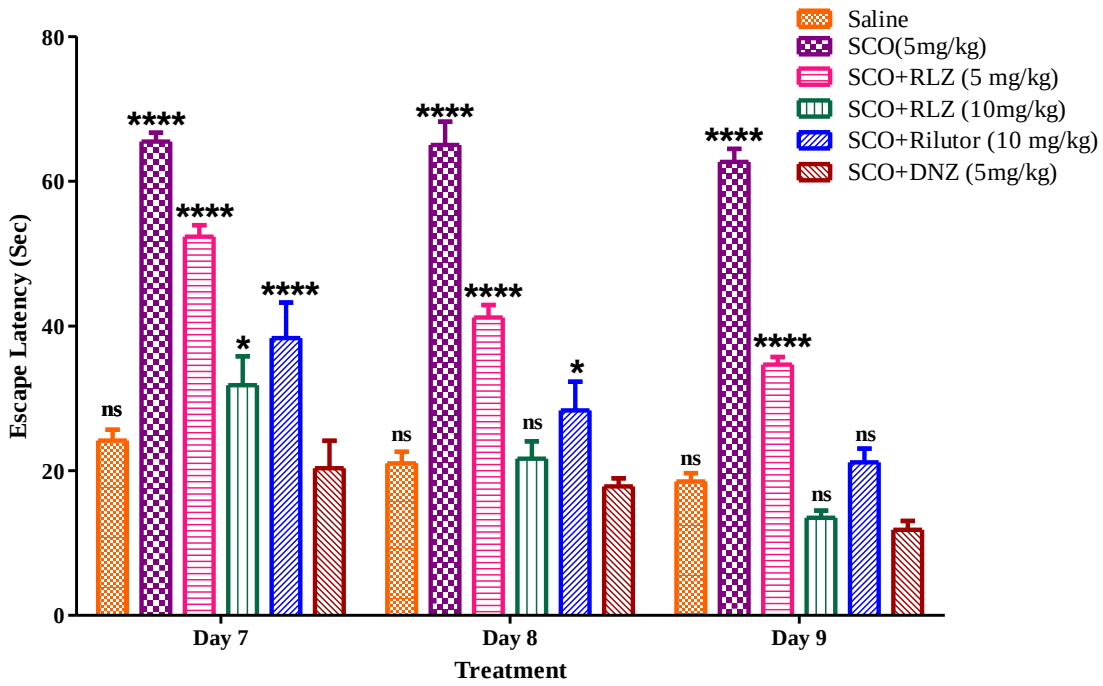

Figure 5.9. Escape latency duration measured in Morris water maze test for different groups of rats. Data represented in n=6 and error bars represent the standard deviation.

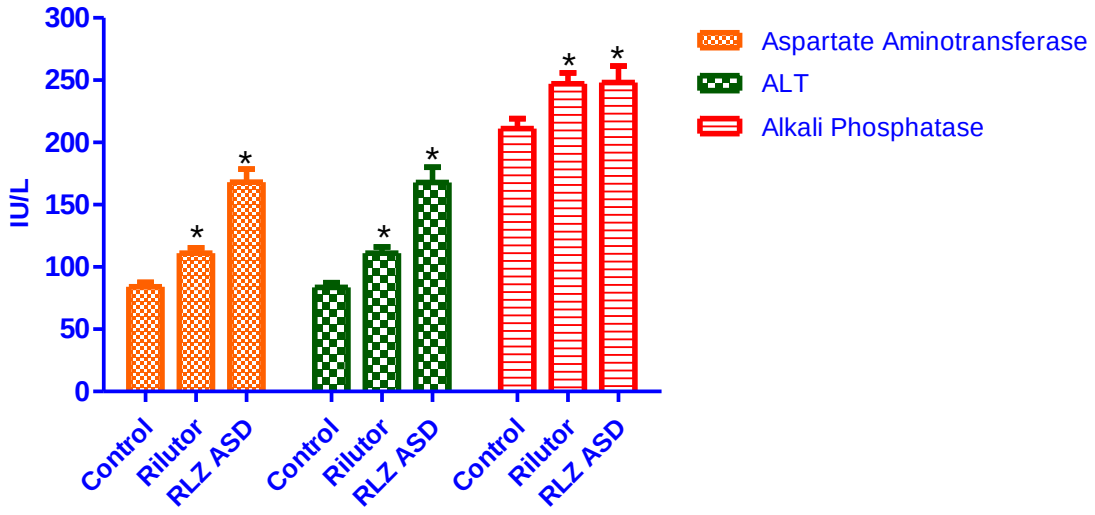

Figure 5.10. Enzyme levels of control group in comparison with Rilutor™ and RLZ ASD at a dose of 10 mg/Kg. Data represented in n=6 and error bars represent the standard deviation.

5.3.7.2 Hepatotoxicity Evaluation

Figure 5.10 shows the comparison between control group, The current study describes that with increased pharmacokinetic profile the hepatotoxicity on the drug is also

increasing. The drug treatment group with Rilutor™ and RLZ ASD at 10 mg/Kg dose shows statisticaly significant increase in the AST, ALT and ALP levels with $p< 0.05$. Riluzole has been found to induce hepatotoxicity, hence restricting its usage. This experiment gives an insight that if dose of RLZ will be reduced in further studies keeping in mind its enhanced pharmacokinetics and pharmacodynamic effect then it can be a promising treatment approach.

5.4 Conclusions

After successful development and characterization of the formulation, PBPK model was developed for tablet and ASD with oral dosing to simulate the RLZ concentration in different organs with time. The model carries the capability to predict both the RLZ and its metabolite RLZ-OH in multiple organs thus enhancing its capacity to predict safety and efficacy in multiple organs. For the sake of simplicity and due to unavailability of data especially V_{max} and k_m, multiple metabolites for the model were not considered. Another aspect worth mentioning is the polymorphic hepatic CYP450 metabolism may lead to more inter-subject variability especially in human [231]. Currently, polymorphism was not considered, but it may lead to some interesting outcomes, for instance, observed hepatotoxicity in specific individuals [267]. Nonetheless, the PBPK model developed here can act as a starting point to explore mechanistic PK for Rilutor™ and RLZ ASD.

The developed PBPK model predicted fairly well for tablet and ASD formulation in rat, however, the limitation was the unavailability of data at multiple doses. Since a similar dose was used for optimizing 3-4 biochemical parameters, considerable uncertainty exists for the robustness of the PBPK model in rats. Nonetheless, the plasma concentration was used for optimizing the rat model, the model showed good prediction in brain as well without any further optimization. For human Rilutor™, the model validity can be

confirmed since after optimizing the model at one dose, it performed well for other dosing scenarios (Figure 5.5b).

The results of this study are promising for PBPK application in dose design especially in the context of target tissue concentration. Interestingly it was observed that C_{max} for ASD was almost double compared to Rilutor™ in brain for the rat with similar trend for human. The increased C_{max} for RLZ ASD points towards increased active concentration in brain for ASD hence may result in improved efficacy. The model developed here can be further used to predict the concentration in urine, feces and also in other organs of human body, thus understanding the toxicity. The current model can also be adapted to large human population by considering the metabolic and genetic diversity which may explain the sensitivity of population towards adverse effects of RLZ. Based on the finding of pharmacokinetic, PBPK modelling, pharmacodynamic and enzyme level studies it can be concluded that to achieve a similar therapeutic effect the dose of RLZ can be reduced. This will help in managing the toxicity associated with this drug and hence increasing its overall safety.